Using Polyalkylene Carbonates (QPAC) as a Binder in Solar Pastes

Sponsored by Empower Materials

Table of Content

Introduction

Over the last two decades, there has been a significant effort to improve reliability, efficiency and manufacturability of photovoltaics (PV). Most of this effort has been targeted towards thePV's front-side construction, including contact formation with glasses and metallization. To that end, extensive advancements have been made to optimize the application of front-side conductive architecture so as to realize the highest quality of end product with superior manufacturing capacities.

Silver pastes are often used on the front-side architecture of a solar cell. These pastes are heterogeneous mixtures comprising of metallic silver flakes or powders, organic binders, glass frits, and other additives like dispersant/surfactants, plasticizers, solvents and the like. The silver-bearing part of the front-side paste constitutes a flake type powder, a spheroidal powder, or a combination of the two. The frit component of the pastes does not contain lead, and provides a range of CTE and Tg, in addition to particle size and distribution. Both the performance and quality of the front-side design of a solar cell are governed by these two material sets.

While the organic phase of the front-side solar paste plays a major role, it is often consigned to the transference of the imparted structural design, and how well the paste is able to process during the course of printing. Although a wide range of materials is available for the organic phase of the front-side solar paste, most commercially available systems only belong to a few categories — acrylics, cellulosics, and rosinates.

Figure 1 illustrates a few basic binder materials together with polypropylene carbonate derived from the polyalkylene carbonate group of materials. The polymeric range can be made to offer different molecular weights, which can impart degrees of control of organic rheology. The rosin range of binders originates from a fundamental building unit of abietic acid. As such, the rosins are often hydrogenated to prevent unsaturation, and are either utilized in this form, or reacted to form different esterified versions of hydrogenated rosins.

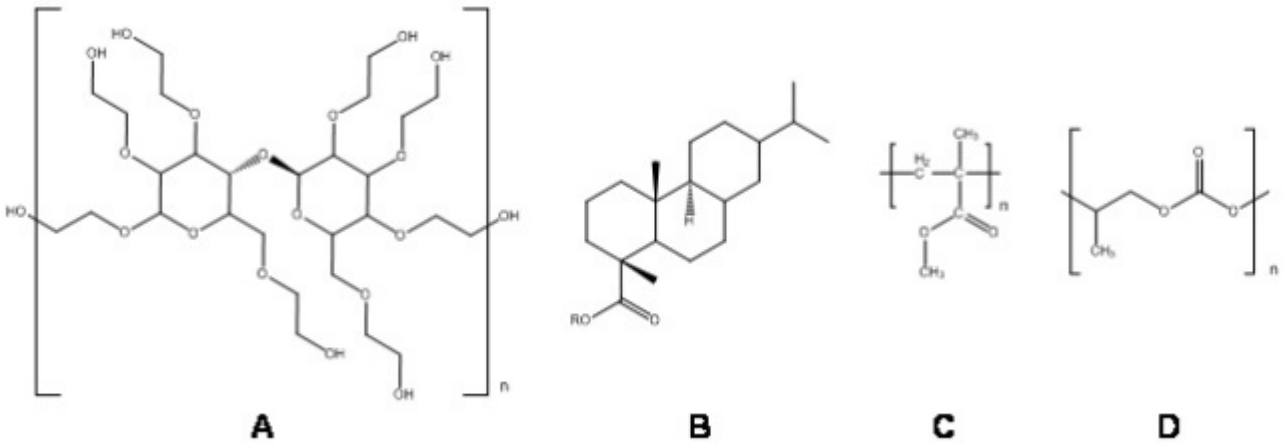

Figure 1. *Chemical structure representations of binder materials for pastes. A: hydroxyethyl cellulose, B: a rosinate, C: an acrylic, D: polypropylene carbonate.*

The general composition of the materials, together with the chemical formula and corresponding degrees of unsaturation are listed in Table 1. The materials' composition andstructure play a major role in how they impart the preferred fluid properties and render the interaction with solid phases in a paste during printing and firing processes.

Table 1. *Hydrocarbon composition of structures of Figure 1*

Material Name	Composition			Chemical Formula	Degrees of Unsaturation
	C (Wt.%)	H (Wt.%)	O (Wt.%		
Hydroxyethyl Cellulose	~48	~8	~44	$C_{14}H_{27}O_{10}$	1.5
Rosinate	~78	~12	~10	$C_{20}H_{34}O_2$	4
Acrylic	~65	~10	~25	$C_7H_{14}O_2$	1
Polypropylene Carbonate	~54	~10	~36	$C_6H_{12}O_3$	1

Generally, rheological characteristics of front-side solar pastes are shear-thinning, non-Newtonian, thixotropic fluids. A paste is formulated by different mixing and milling processes, integrating individual components to obtain the required viscosity response with related solids content, and at the same time acquiring controlled and repeatable performance during the application and processing protocols. This article aims to show the drop-in-replacement compatibility of a clean-burning binder systems, with traditional material sets to manufacture PV cells that are similar to existing modern expectations.

Experimental Procedure

A thick film paste was used to assess a finished PV cell. This paste was developed from QPAC40,a polycarbonate-based binder system from Empower Materials. For the additional solvent, propylene carbonate was used. Then, using a mixture of spherical and flake powders (PV-2 and SF-3), the silver phase of the clean-burning binder paste was made. Dispersing agents and plasticizer were used to provide excellent paste properties and processability. A lead-free glass composition was also used. Table 2 shows the composition of the thick film paste used in this analysis.

Table 2. *Thick film paste composition with clean-burning binder*

Component Name	Composition (Wt.%)
Silver	86.2
Glass	4.5
Dispersant & Plasticizer	3.7
QPAC40 Binder	3.6
Solvent	2.0

In order to develop the QPAC40-based binder paste system, the silver components were mixed with the solvent, plasticizer, and dispersant by means of a non-contact planetary mixer. Once the initial mixing was complete, the QPAC40 binder solution was introduced, and the mixing program was performed again. As soon as the second mixing process was over, the glass component was added and the mixing program was again repeated for 12 minutes. The finished paste was simultaneously assessed and compared with other commercially available systems, designated as Paste A and Paste B.

A Brookfield Engineering HBTD, equipped with a cone and plate type spindle (CP-52), was used to determine the paste quality metrics at 25 °C for stress and viscosity, and a Hegman Gaugewas used for fineness of grind (FOG). Next, thermal analysis was carried out by means of aMettler Toledo STAR TGA/DSC at 10 °C.min^{-1} in air with ceramic pans, and screen printing was carried out with a Baccini Softline printer with speed of 100 mm.s^{-1}, squeegee pressure of 75 N, and snap off of 1.2 mm. Printing was done on 239 cm^2 mono-Si wafers, and all samples were applied with commercial rear tabbing pastes. Firing was done using the model CF-SL six-zone oven supplied by Despatch Industries.

Series Resistance, Efficiency, Solar cell V_{OC}, I_{SC}, FF, and Shunt Resistance were determined by means of a Solar Cell I-V Curve Measurement System IV16L with a class-AAA solar simulator, equipped with continuous 16 x 16 cm beam, Air Mass 1.5 Global (AM1.5G) spectral filtering. The entire cell measurements were carried out after calibration with the National Renewable Energy Laboratory-certified solar cell.

Results and Discussion

Paste Fabrication and Characterization

There are several preferred features for a thick film paste to be used for front-side PV. These features include dispersion stability, material component homogeneity, high solids content, screen printing performance, and rheology. These are all interrelated parameters which prove useful for determining the paste quality for its desired application. The FOG of individual paste system is compared in Table 3.

Table 3. *FOG comparison of paste samples*

FOG Parameter	Paste Sample		
	QPAC	A	B
1st Scratch (µm)	5.5	8.3	5.5
3rd Scratch (µm)	4.2	4.1	5.3

Main Break	1.4	2.1	1.8

These results demonstrate that these pastes are roughly the same with respect to their dispersion state. Standard methods used for producing front-side solar pastes feature a milling step that is done with three roll milling. A non-contact planetary mixer method (Thinky AR250) was used to develop the QPAC40 paste. The FOG results thus obtained demonstrate that end processing of the components for the QPAC40 paste is perfect for the paste fabrication process. The final rheology of the pastes was very similar, as shown in Figure 2 which compares the stress and viscosity responses of the final pastes. A subtle variation was seen in the viscosity responses between the 'A' and QPAC40 samples when compared to the 'B' sample over a 0.25 s^{-1} shear rate, whilst significant variations were seen in the stress responses of each individual paste sample. This is due to the presence of different components in the pastes, such as glass materials, variations in particle shape and size of the silver powder, other additives, and the general organic composition.

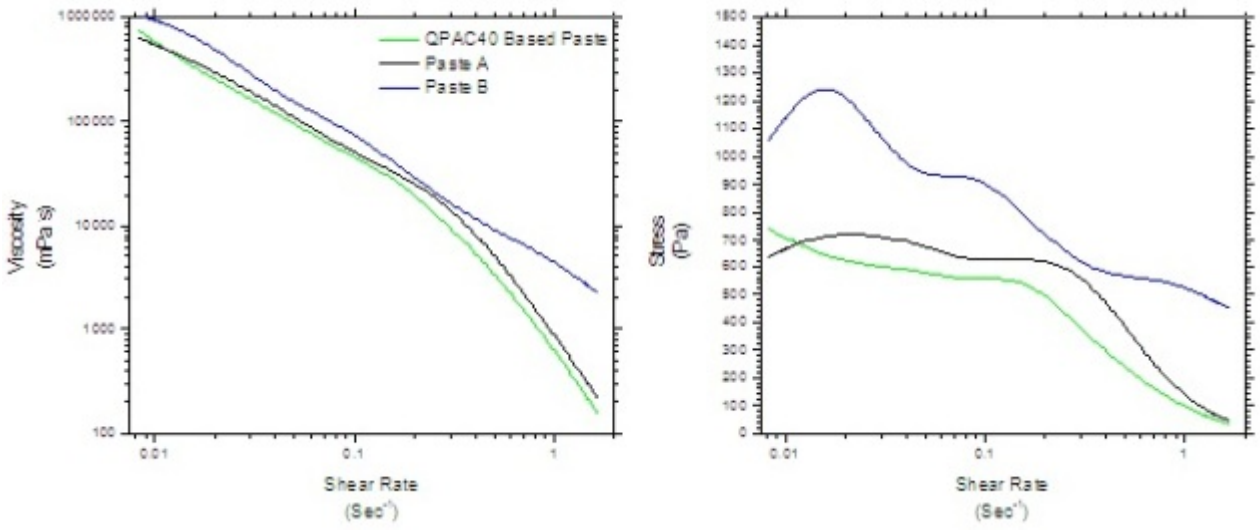

Figure 2. *Viscosity (left) and Stress (right) vs. shear rate of each thick film paste.*

The organic components of thick film pastes applied on the front-side architecture of the solar cell were predicted to allow retention of the imparted geometry, but were fully removed during the course of the firing process so that both the metal and glass could reach their optimal final phase without impacting the mechanisms of phase formation. Figure 3 shows the differential scanning calorimetry (DSC) and thermogravimetric analysis (TGA) responses of the individual pastes assessed in this analysis.

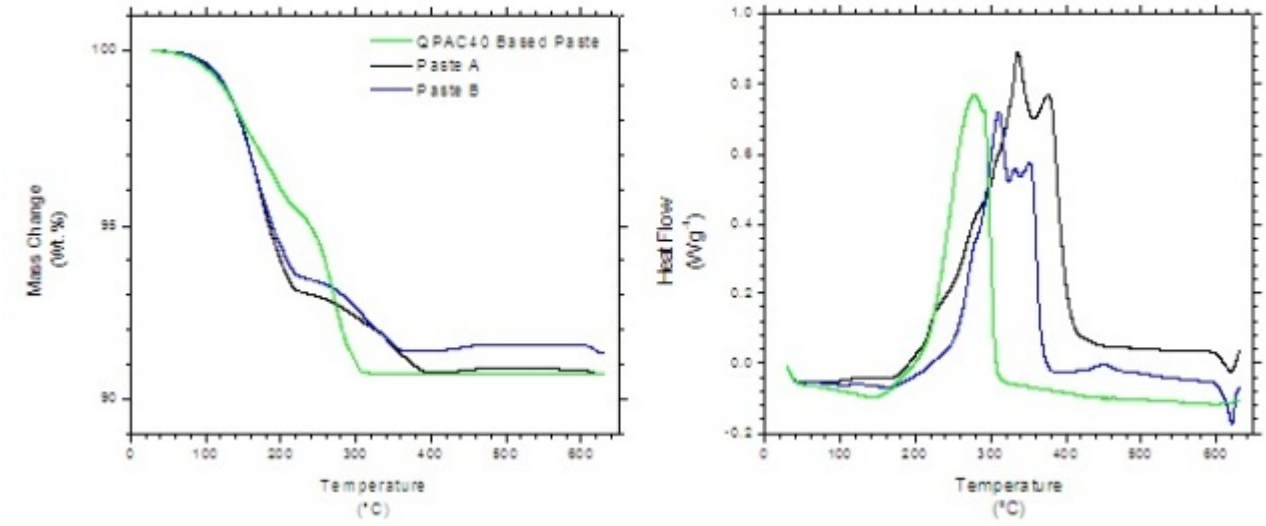

Figure 3. *TGA (left) and DSC (right) traces of each thick film paste. Thermal scan performed in air at 10 °C.min^{-1}.*

It was observed that each paste had analogous properties with regards to the loss of solvent and other onsets of organic component decomposition. Overall mass changes were also similar, but did not occur in the same temperature region. Paste A and B exhibited on-going mass loss as a result of decomposition until ~400 °C, while the QPAC40 based paste exhibited almost complete removal at 300 °C temperature. Extensive retention of organic decomposition was seen in Paste A and B TGA traces to over 650 °C. Table 4 shows the comparison of mass changes for all pastes at 50 °C increments from 300 to 630 °C.

Table 4. *TGA summary of thick film paste comparison*

Temperature (°C)	QPAC40 Paste Mass (Wt.%)	Paste A Mass (Wt.%)	Paste B Mass (Wt.%)
RT	100.0	100.0	100.0
300	91.0	92.3	92.6
350	90.7	91.5	91.6
400	90.7	90.8	91.4
450	90.7	90.8	91.5
500	90.7	90.9	91.5
550	90.7	90.9	91.5
600	90.7	90.8	91.5
630	90.7	90.7	91.3

While similarity was again observed in the shape of the heat flow curves obtained from the thermal decomposition analysis of individual paste sample, the heat flow energy failed to occur in the same thermal region. In the QPAC40 based paste, an exothermic peak was seen at 280 °C, while in Paste A and B, exothermic excursions were seen at 335 °C and 310 °C, respectively, along with extra decomposition daughter exotherms

over these temperatures. Finally, both Pastes A and B had a signal of about 600 °C, relating to a TGA mass loss of 0.1 to 0.2 Wt.%, showing intense carbonaceous residue experiencing final decomposition in the thermal profile. The heat flow data shows the differences of individual paste sample experiencing the same thermal profile (Figure 4).

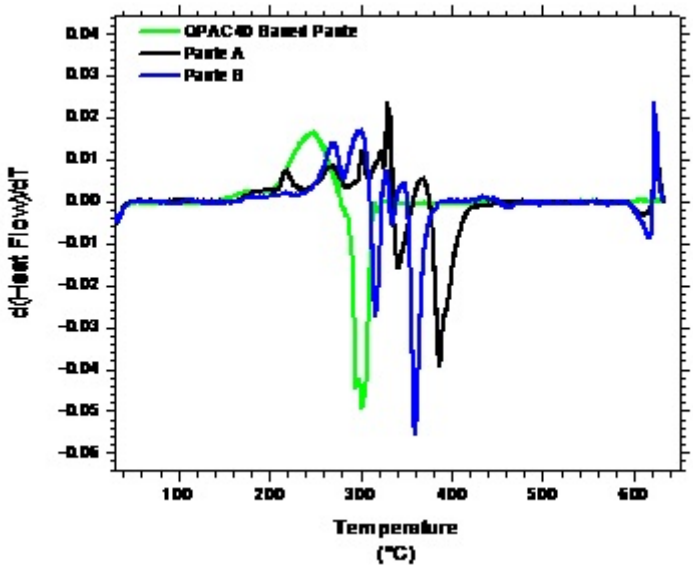

Figure 4. *Representation of the rate of change of energy during exposure of each paste sample to the same linear thermal profile in air.*

Cosmetics and Microstructure

Scanning electron microscopy of the finger lines and bus bars was done on the planar view of the fired and printed wafers, and the same was done on the fracture cross sections of the finger lines. The same areas of bus bars and finger lines were investigated from individual set of fired and printed wafers representing individual paste types. The representative images from these results are shown in Figure 5. From Column 1 and 2 images, it is possible to determine the line widths as 84 µm, 95 µm and 105 µm for the QPAC based paste, Paste A, and Paste B respectively. When the finger lines and bus bars were subjected to high magnification analysis, a major difference was seen in the pore/void concentration on the fired and printed surface features of each individual paste sample (Column 3, Figure 5). In the final bulk lines of individual paste sample, no major cosmetic differences were observed.

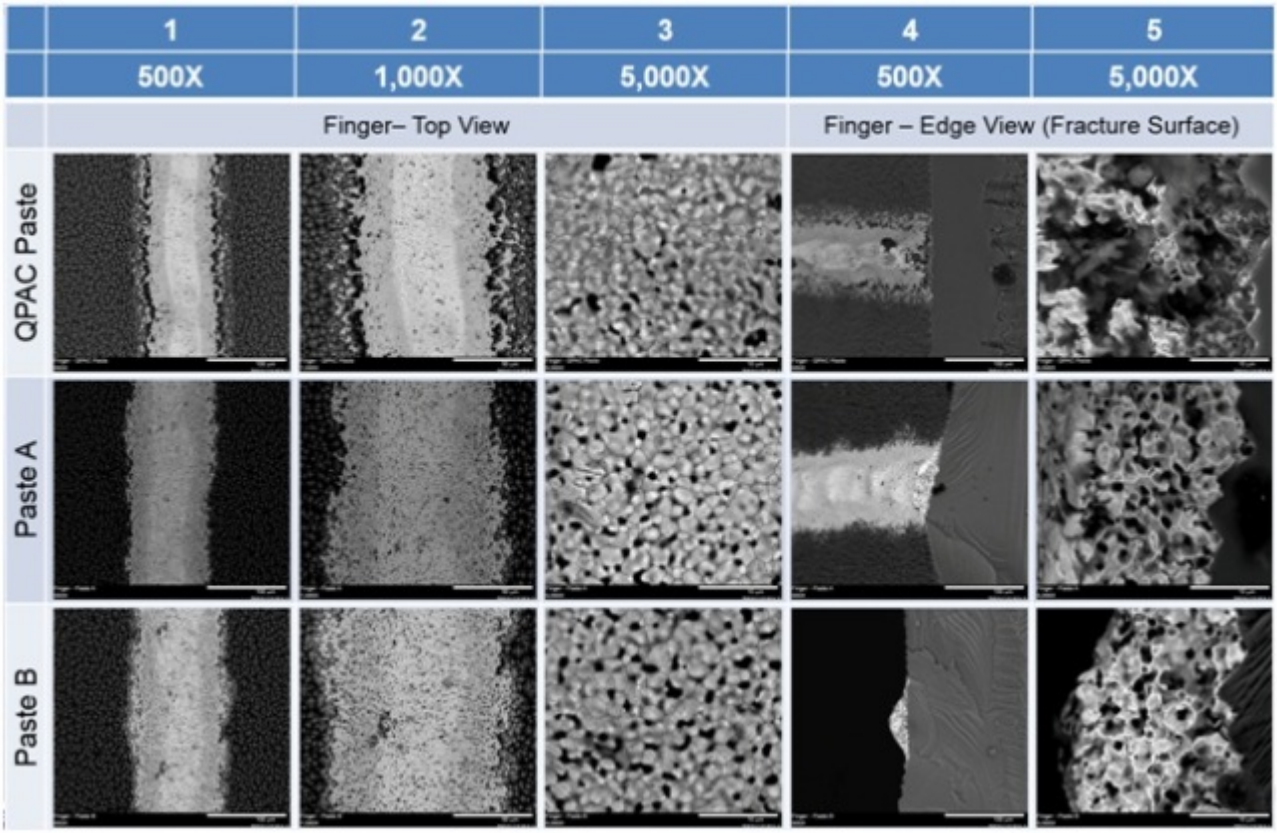

Figure 5. *SEM images of finger lines from each paste (after firing).*

The finger lines' fracture-cross sections from individual paste sample are illustrated in Columns 4 and 5 of Figure 5. In fact, the 5,000X magnification images seen in Column 5 show marked variations between Paste A and B and the QPAC40 based paste. In Paste A and B, intensive cross section pore/void spaces are seen in the finger line body spanning from the wafer interface to all surfaces of the finger line. Conversely, superior interface properties are seen in both Paste A and B between the wafer and the conductive finger line. In the case of the QPAC40 based paste, no pore/void space is seen in the finger line body, but poor interfacing are seen at the wafer interface and conductive finger line.

Electrical and Reliability Testing

The electrical testing data of individual pastes compared in this analysis is shown in Table 5. The 'Suns-V_{OC}' data shows closely similar results of individual paste samples in this analysis.

Table 5. *Summary of electrical testing results*

Parameter	Units	Sample		
		QPAC40 Based Paste	Paste A	Paste B
Suns-V_{OC}				
Pseudo Efficiency	(%)	18.0%	18.5%	18.5%
pFF	(%)	79.4%	81.3%	81.0%
R_{SHUNT}	(Ω cm^2, Fitted)	1952.7	150000	4031

Ideality Factor	1 Sun	1.01	1.08	1.08
	0.1 Sun	1.60	1.16	1.24
J_{O1}	($A.cm^{-2}x10^{-12}$)	2.20	2.20	2.10
J_{O2}	($A.cm^{-2}x10^{-12}$)	6.70	3.10	3.16
Contact Resistance				
Sheet Resistivity	(Ω/sq)	73.2	74.1	73.7
Contact Resistance	(Ω)	14.85	0.03	0.02
Transfer Length	(cm)	0.2014	0.0004	0.0004
Contact Resistivity	($\Omega\ cm^{-2}$)	2.96769	0.0001	0.00001
Fit	R2	0.997	1.000	1.000
Light I-V Performance				
V_{Oc}	(V)	0.608	0.615	0.613
J_{SC}	($mA.cm^{-2}$)	37.65	36.61	36.35
FF	(%)	66.7	78.7	79.6
Efficiency	(%)	15.29	17.70	17.74
R_{SERIES}	($\Omega\ cm^2$)	2.88	0.65	0.54
R_{SHUNT}	($\Omega\ cm^2$)	8433	2385	1218

The 1-Sun Ideality Factor or M-Factor indicates better performance in comparison to either Paste A or B, showing stronger junction etching with respect to the QPAC based paste sample. The 'Contact Resistance' results summarized in Table 5 revealed reproducible junction sheet resistance, but the resistivity and contact resistance display poorer performance when compared to Paste A or B. This data shows that the QPAC40 Paste sample did not diffuse into the wafer adequately, and thus confirmed the above-discussed SEM results. Paste A and B showed excellent performance. Similarly, the QPAC40 paste sample had desirable characteristics, but reduced junction etching.

Conclusion

The front-side solar cell thick film paste sample was developed using a clean-burning binder system. The properties of the pastes were compared with other pastes that are commercially available in the market, and were found to have almost identical properties, such as FOG, rheology, and solids loading. Thermal analysis of the commercial systems, in contrast to the paste sample, showed that the former had a wide decomposition range and the presence of residual carbonaceous material as high as 630 °C, while the QPAC40 based paste offers complete organic phase burn-out by 300 °C in air. Comparison was also made of the final microstructure and cosmetic features of the fired and printed structures on the front-side of solar cells. While the commercial paste samples were similar to each other in terms of electrical testing, the QPAC40 based paste exhibited excellent qualities but showed poorer electrical performance as a result of reduced junction etching. However, if a different glass component is used in the formulation, this limitation can be resolved.

EMPOWER MATERIALS

This information has been sourced, reviewed and adapted from materials provided by Empower Materials.

For more information on this source, please visit Empower Materials.